PROPER INTERPRETATION OF FREEZING AND HYDRATE PREDICTION RESULTS FROM PROCESS SIMULATION

Michael W. Hlavinka, Ph.D., P.E.
Vicente N. Hernandez, Ph.D.
Bryan Research & Engineering, Inc.
Bryan, TX , U.S.A.

Dan McCartney
Black & Veatch Energy
Overland Park, Kansas, U.S.A.

ABSTRACT

This paper focuses on the modeling of solid phase behavior in systems that are frequently encountered in natural gas processing. The ability to perform accurate calculation of freezing or solids formation conditions in processes from dry ice, hydrates, and water ice is quite important. Although the primary focus in this work is on dry ice formation from carbon dioxide, analogies with hydrate formation are presented. A description of the phase equilibria at different conditions of temperature and pressure is included. The paper compares the predicted results from simulation with selected experimental data sets, and illustrates that accurate results are obtained over a wide variety of conditions. However, due to the complicated phase behavior of these systems, improper interpretation of results, or incorrect use of the tools within the simulator is possible due to the multiplicity of incipient formation points. One fact that is not well known is that lowering the temperature may cause a solid that has formed to melt under certain conditions of pressure and composition. While recent work has been done to mitigate the incorrect application of these tools, knowledge of some of the different types of phase behavior is generally desirable to understand and exploit the results. Phase diagrams are presented to aid in understanding the solid formation behavior.

PROPER INTERPRETATION OF FREEZING AND HYDRATE PREDICTION RESULTS FROM PROCESS SIMULATION

INTRODUCTION

The accurate prediction of the formation conditions of solid species is commonly required in process simulation. In gas processing, the most common solid forming species are dry ice from carbon dioxide (CO_2), and hydrates and ice from water. Dry ice formation can occur in cryogenic gas processing as in turboexpander plants where methane (CH_4) is typically separated from heavier paraffinic natural gas components. In particular, the top trays and the associated draws and feeds of the demethanizer in these facilities are particularly susceptible to dry ice formation when CO_2 is present due to the low temperature conditions present on these trays. Water ice can also form in natural gas processing. Dry ice and water ice form a virtually pure CO_2 and water solid phase, respectively. Due to the increase in volume on freezing of ice and the associated negative slope of the melting point line on a pressure-temperature diagram for water, ice cannot exist as a pure phase above its triple point ($32.018°F/0.01°C$). Ice will never appear in a process that is warmer than the water triple point temperature. Carbon dioxide exhibits a decrease in volume on freezing, and consequently a positive slope for the melting point line on its pressure-temperature diagram. While it is possible for dry ice to form above the triple point temperature ($-69.826°F/-56.57°C$), dry ice normally forms below this temperature in gas processing.

Hydrates are a particular type of solid species known as a clathrate. Hydrates enclose a guest molecule in a solid water cage, and consequently do not precipitate as a pure solid compound. While hydrates are a significant problem for gas transport in pipelines, they can form any time a hydrate forming guest species and enough water are present, and the temperature and pressure are in the hydrate formation region, which can be above the freezing point of water. In gas pipelines, enough water is frequently present to form hydrates at ambient temperatures and pipeline pressures.

In this paper, we will demonstrate that accurate predictions of solid forming conditions across all regions are provided by ProMax®, the general purpose process simulator by Bryan Research and Engineering, Inc. While ProMax generally offers improved predictions over its predecessor PROSIM®, the predictions from PROSIM were also good. Recent papers [1, 2] have suggested that unreliable results for dry ice formation conditions were prevalent in several commercial simulators. Although this may appear to be true at first inspection based on the results of their presentation, in actuality the values are reliable when using ProMax and PROSIM for solid formation from a system comprised of vapor and liquid (including immiscible liquids) phases if the tools are applied in the context for which they are designed. The authors are not drawing any conclusions or inferences regarding the results or behavior of the tools present in any other process simulation program. Unfortunately, misapplication of the results is possible if familiarity with the complex phase behavior of these systems is not considered. We have attempted to revise the presentation within our newer ProMax software to prevent incorrect application of its solid formation calculations. However, even with these efforts in program revision to remove ambiguity, we feel that writing this paper is necessary to minimize the likelihood of inappropriate application of results. Without a fundamental understanding of the phase behavior, inappropriate application is still possible.

The solid formation utilities available in ProMax and PROSIM are quite complete. Solid formation temperature can be calculated from stream overall or individual phase composition and pressure through a dedicated stream utility. Additionally, the incipient conditions are calculated by a

separate phase envelope utility for tabular and graphical display. In order to prevent modeling a system that would operate in a solid region, the program checks for incipient formation conditions in every unit operation and stream in a simulation. This also includes every stage of a distillation column, as well as internal increments within heat exchangers. An appropriate warning indicating the location of the solid formation condition is issued if operation occurs within a user defined threshold.

While most of this paper focuses on CO_2 dry ice formation in a binary mixture with methane, the same fundamental principles apply to dry ice, ice, and hydrate formation in more complex systems. Since similar phase behavior is also present in these systems, the results from these simulations should be analyzed in a similar manner.

THERMODYNAMIC REVIEW

From thermodynamics, a system of N components at a given temperature and pressure is in equilibrium when the chemical potentials for each component in all phases are equal. Mathematically this can be expressed as:

$$\mu_i^\alpha = \mu_i^\beta = \cdots = \mu_i^\pi \qquad (i = 1,2,...,N) \tag{1}$$

where μ_i^α represents the chemical potential of component i in phase α. The chemical potentials are a function of temperature, pressure, and phase composition. For a system forming vapor, liquid (single), and solid phases, equation (1) can be written as:

$$\mu_i^V = \mu_i^L = \mu_i^S \qquad (i = 1,2,...,N) \tag{2}$$

where V, L, and S represent the vapor, liquid, and solid phases, respectively.

When CO_2 is the solid forming component, the solid exists as pure CO_2, and the equations for this system are:

$$\mu_i^V = \mu_i^L \qquad (i \neq CO_2) \tag{3a}$$

$$\mu_{CO_2}^V = \mu_{CO_2}^L = \mu_{CO_2}^S \tag{3b}$$

Here, $\mu_{CO_2}^S$ represents the chemical potential of pure CO_2 as dry ice at the temperature and pressure of the system. For simplicity, if we restrict our analysis to a binary system of CH_4 and CO_2, the following equations are applicable depending on the phases present:

Methane	Carbon Dioxide	Phases Present
$\mu_{CH_4}^V = \mu_{CH_4}^L$	$\mu_{CO_2}^V = \mu_{CO_2}^L = \mu_{CO_2}^S$	V,L,S
N/A	$\mu_{CO_2}^L = \mu_{CO_2}^S$	L,S
N/A	$\mu_{CO_2}^V = \mu_{CO_2}^S$	V,S

Again, the CO_2 chemical potential for the solid phase is a pure component chemical potential, while the chemical potentials of the liquid and vapor phases are mixture properties, dependent on phase composition.

The equations for chemical equilibrium (Equation 1) result from the equilibrium requirement of the minimization of the total free energy of the system. Any other phase composition combination other than the equilibrium composition will result in a higher free energy than the equilibrium

composition. Additionally, a phase (vapor, liquid or solid) will only form (or disappear) if it lowers the free energy of the system, driving the system to a minimum free energy level. Therefore, dry ice only forms when its presence will lower the total free energy of the system.

A qualitative phase diagram for the CH_4-CO_2 binary system is presented in Figure 1. In this figure, the overall composition of the system is constant. The phase rule indicates that the number of degrees of freedom for a two phase binary system is two and one for a three phase system. Therefore, the three phase region of any binary system is depicted by a line in Figure 1. The system is univariant along this line. Fixing the temperature, not only fixes the pressure, but also the composition of the vapor and liquid phases. The overall composition is not fixed, but can vary in a manner that preserves mass balance. Derivatives of thermodynamic properties along this line are total derivatives. Within the two phase regions, the system requires two variables to be specified in order for it to be completely determined. Therefore, the two phase regions result in areas in Figure 1. Partial derivatives of thermodynamic properties can be evaluated in the two phase and single phase regions.

The locus of all three phase solid-vapor-liquid equilibrium points in the CH_4-CO_2 binary system is represented by line BDF in Figure 1. Lines FH and FG are also three phase lines, but are not
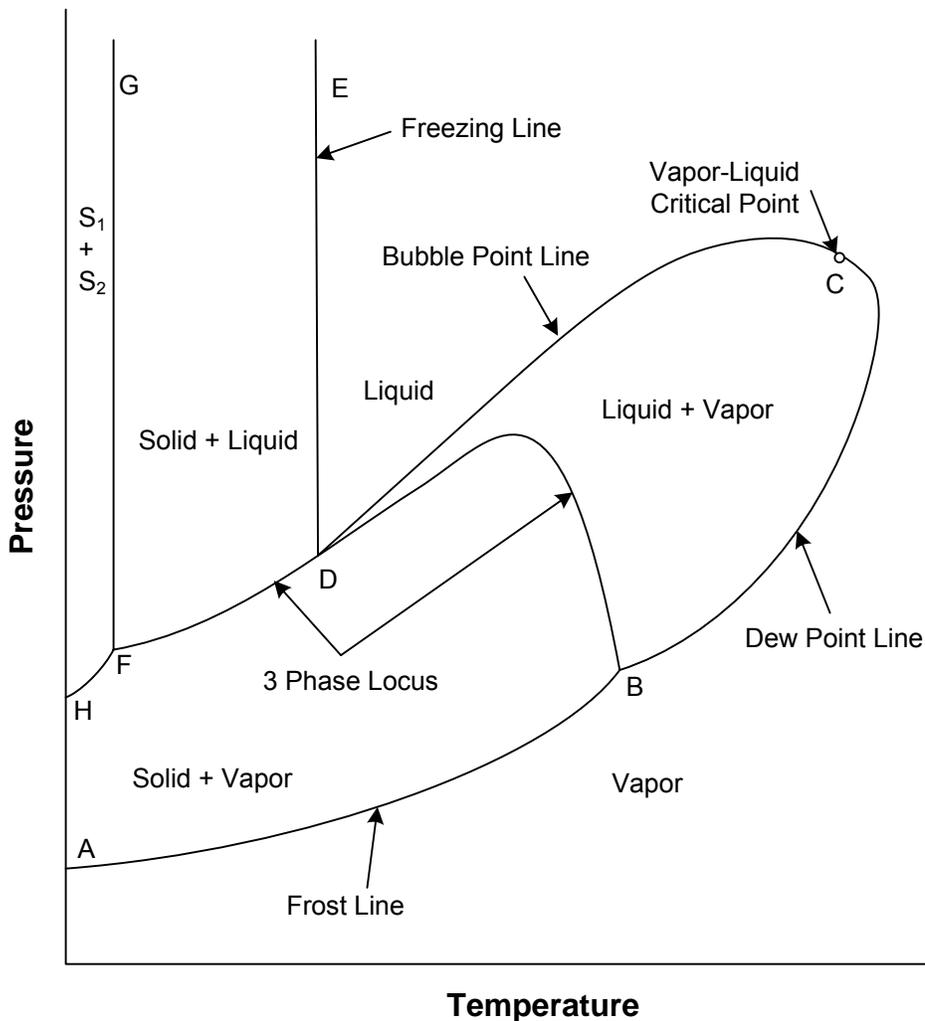

Figure 1. Qualitative Pressure-Temperature Diagram for the Methane-Carbon Dioxide Binary System.

discussed in this presentation because they are at temperatures where methane freezes as a separate solid phase. Line AB is the boundary between the vapor and solid-vapor region. This line is frequently called the frost or snow line. Line BC represents the dew point line separating vapor from the vapor-liquid region, and CD represents the bubble point line separating liquid from the vapor-liquid region. Point C is the mixture vapor-liquid critical point. Line DE separates the liquid region from the solid-liquid region. This line can be called the freezing or melting line. If the overall composition of the mixture is changed, the location of the lines AB, BC, CD, DE, and point C will change. However, due to the univariant nature of the three phase locus for a binary system, the three phase boundaries will not change position because their coordinates are fixed on a pressure-temperature diagram. Changing the overall composition will only affect where the dew and bubble point lines intersect the three phase locus at points B and D.

Figure 2 presents the three phase locus and dew, bubble, frost, and freezing lines for 10% and 50% (molar) overall compositions of CO_2 in CH_4, in addition to the pure CO_2 and CH_4 lines as generated by ProMax. This figure expands upon the qualitative diagram presented in Figure 1 by including more than a single composition. Exclusive views of the 10% and 50% CO_2 systems are presented in the top and bottom inserts of Figure 2, respectively. From Figure 2, it can easily be seen that cooling a system of fixed composition at constant pressure can result in crossing phase boundary lines that include solid phases multiple times depending on composition and pressure combinations. For example, cooling the 10% system along a 600 psia (41.4 bar) isobar from 100°F (38°C), a frost line is first encountered at -92.6°F (-69.2°C), the three phase locus at -114.1°F (-81.2°C), and the freezing line at -117.8°F (-83.2°C). The bubble point line is also crossed at -114.8°F (-81.6°C), between the three phase locus and freezing line. At temperatures between the three phase locus and the freezing line, no solid is present. The solid CO_2 that formed at temperatures between the frost line and three phase locus has been dissolved by the liquid. Only temperatures below the freezing line cause the solubility of the CO_2 in the liquid to be low enough to freeze as a separate solid phase.

The same cooling process of the 50% line along a 600 psia isobar indicates that the dew point is first encountered at -11.8°F (-24.3°C). The three phase locus is crossed at -83.7°F (-64.3°C) and -114.1°F (-81.2°C). Between these temperatures, the system is a solid-vapor system. All liquid that has been created between the dew point and upper three phase point has frozen. Below -114.1°F (-81.2°C), the system is a solid-liquid system, until at some lower temperature as indicated in Figure 1, the entire system solidifies.

Figure 3 illustrates the dimensionless chemical potential difference between CO_2 in the most stable phase (vapor, liquid, or both ignoring the presence of solid) and CO_2 in dry ice as a function of temperature at 600 psia (41.4 bar) for binary mixtures of 0.1%, 1%, 10%, and 50% CO_2 in methane as generated by ProMax. If both vapor and liquid phases are present, the chemical potential in the vapor and liquid phases are equal as required by equilibrium. From equation 3b, it is obvious that when this chemical potential difference is zero, the system will form dry ice. This occurs when the lines in Figure 3 cross the temperature axis. Moving from high temperature to low temperature along the 0.1% CO_2 line illustrates what appears to be a function discontinuity at approximately -123°F (-86.1°C). In fact, the function is continuous across the entire temperature range, but instead has two near discontinuities in the first derivative, at the top and bottom of the peaks. The top and bottom occur at the dew and bubble points, respectively. The fact that the temperatures at the top and bottom are very close to one another is indicative of the composition of the mixture. The system is nearly pure methane, and consequently behaves as a near pure component where the dew and bubble points are equal, resulting in a complete transition from vapor to liquid over a small temperature range. Consequently, the system has near discontinuities in chemical potential derivatives just as a pure component has true discontinuities at the boiling (and melting) point. For pure compounds, these
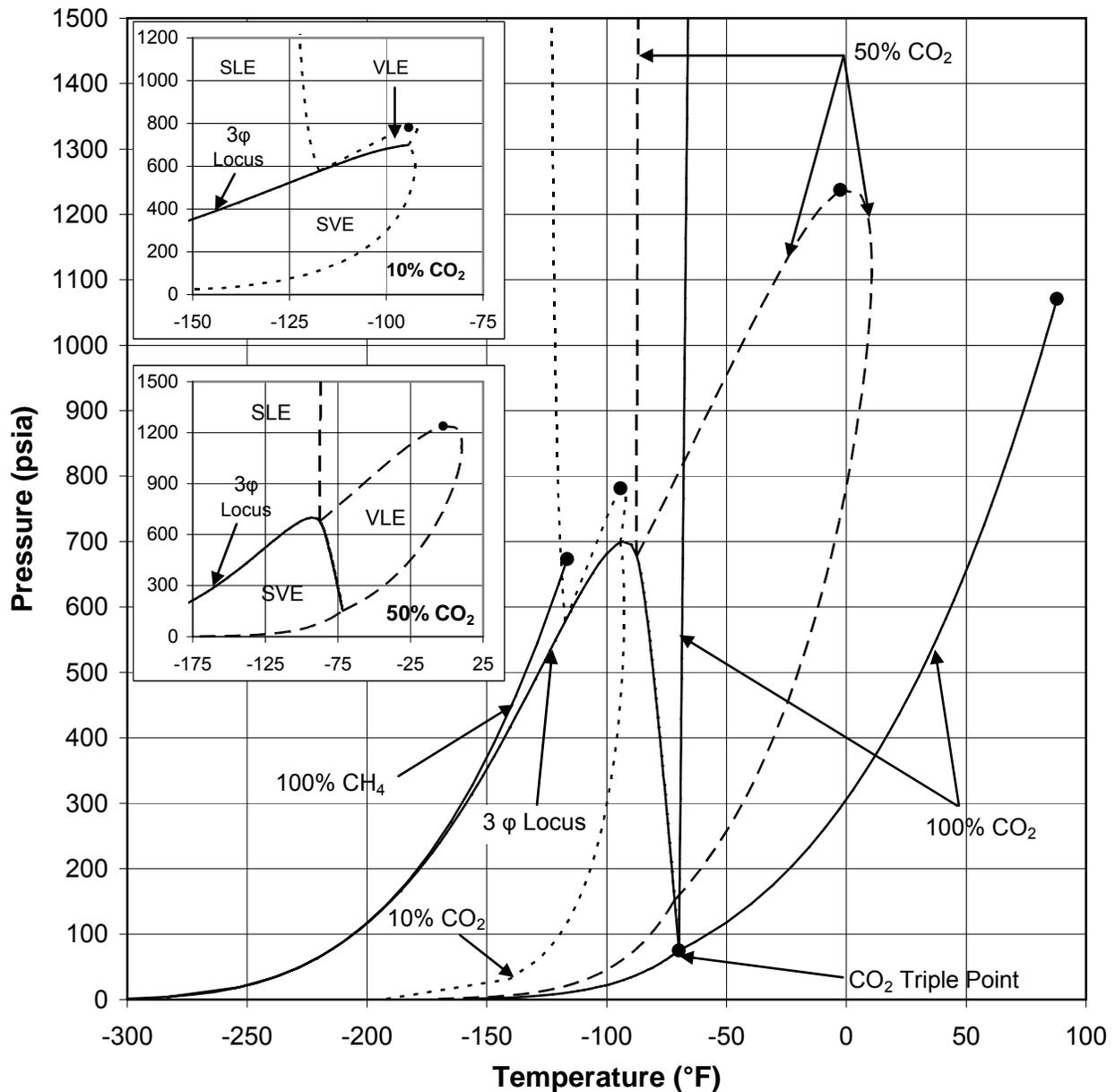
Figure 2. Pressure-Temperature Diagram for the 0%, 10%, 50%, and 100% Carbon Dioxide in Methane Binary System.

discontinuities are frequently called first order transitions because the first order derivatives are discontinuous. Normally, first order transitions exhibit large changes in enthalpy, entropy, and volume across the transition, the first derivative properties of chemical potential. As discussed earlier, the 50% line exhibits a dew point at -11.8°F (-24.3°C) and shows a much more gradual change due to its more mixed character, without approaching derivative discontinuity.

The 0.1% CO_2 system crosses the temperature axis at approximately -233.2°F (-147.3°C), below the bubble point temperature indicating the system in a solid-liquid region (no vapor). The three crossings of the 10% system, -92.6°F (-69.2°C), -114.1°F (-81.2°C), and -117.8°F (-83.2°C), shown in
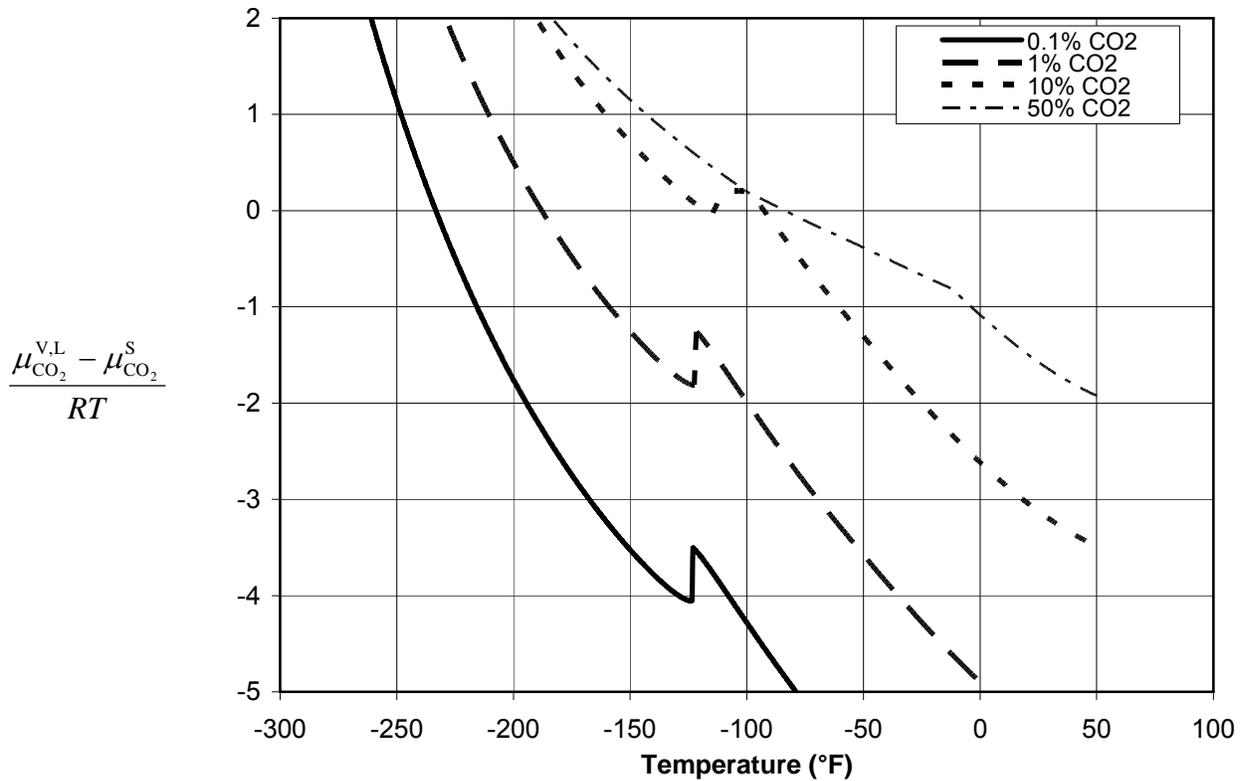
Figure 3. Dimensionless CO$_2$ Chemical Potential Difference at 600 psia (41.4 bar).

Figure 2 are also evident in Figure 3. The -92.6°F temperature is above the dew point indicating the system is in the solid-vapor region, the -114.1°F point is between the bubble point and dew point indicating a solid-vapor-liquid region, and the -117.8°F point is below the bubble point indicating a solid-liquid region. As this system is cooled isobarically at 600 psia, the system begins to form dry ice at -92.6°F, begins to melt the dry ice from liquid formed as the system is cooled below the dew point until all solid is gone at -114.1°F, and then forms dry ice again at -117.8°F as the liquid loses its capacity to carry liquid CO$_2$. The system actually forms dry ice as the temperature is raised from -114.1°F.   At temperatures below -117.8°F, the system is a solid-liquid system until at some temperature the entire system freezes into two solid phases, one virtually pure CH$_4$, the other virtually pure CO$_2$. The 50% system intersects the temperature axis at -83.7°F (-64.3°C), below the dew point, also evident from Figure 2. From the discussion of Figure 2, this point is a transition from a vapor-liquid region to a solid-vapor region. In reality, the 50% line will also intersect the axis at -114.1°F, but this represents an SVE to SLE boundary, a transition which is not calculated by the ProMax utility. When the chemical potential difference is positive, $\mu_{CO_2}^{V,L} > \mu_{CO_2}^{S}$, thus dry ice is stable because its free energy is lower. Conversely, when the chemical potential difference is negative, $\mu_{CO_2}^{V,L} < \mu_{CO_2}^{S}$, thus dry ice will not form because its presence results in a higher free energy level.

COMPARISON AND MODELING OF SELECTED SYSTEMS

Binary Methane-Carbon Dioxide Mixture

Three primary sources of experimental equilibrium data exist that include the solid phase region for the CH_4-CO_2 binary system. The first set of data was acquired by Donnelly and Katz [3]. These data also include vapor-liquid equilibrium data for the system. They measured the three phase locus over the temperature range of -109.5°F to -72°F (-78.6°C to -57.8°C). Their data also included four points in the SLE region and a single SVE measurement. Later, Pikaar [4] presented a fairly extensive set of data for the system. Pikaar used a constant volume cell to measure the saturation pressure of pure methane, and the 1%, 3%, 5%, 10%, and 20% CO_2 frost lines, as well as segments of the dew and bubble point lines for these mixtures in the vicinity of the three phase locus. Pikaar also measured three phase locus points using the constant volume cell over a range of approximately -202°F to -99°F (-130°C to -73°C). Using a saturation cell, Pikaar measured solid-vapor equilibria along -81.4°F (-63°C), -94°F (-70°C), -112°F (-80°C), -130°F (-90°C), -148°F (-100°C), -184.5°F (-120.3°C), and -220.9°F (-140.5°C) isotherms. Additionally, solid-liquid equilibria along -112°F (-80°C), -119.2°F (-84°C), -130°F (-90°C), -148°F (-100°C), -184.5°F (-120.3°C), -220.9°F (-140.5°C), and -255.3°F (-159.6°C) isotherms were acquired in the saturation cell. Finally, Davis et al. [5] measured the three phase locus from -284.1°F (-175.6°C) to near the triple point of carbon dioxide. Additionally, Davis et al. sampled the vapor and liquid phases for composition analysis at points along the three phase locus. No data in the SVE or SLE regions were acquired.

The Davis et al. data cover the widest temperature range measured for the three phase locus, and include the regions measured by Pikaar and Donnelly and Katz. The Donnelly and Katz data are at higher temperature, indicating higher levels of carbon dioxide in the methane. It should be noted that there is a serious discrepancy between the Donnelly and Katz data, and the Davis et al. and Pikaar data for the three phase locus in the lower temperatures measured by Donnelly and Katz (below -93.5°F/-69.7°C). This discrepancy has been discussed by Pikaar and Davis et al., in addition to Sterner [6]. The agreement between the data sets is much better at the higher temperatures. Professor Katz acknowledged that he had reason to question some of the lower temperature data after they were published [7].

Figure 4 presents the three phase locus generated by ProMax, with experimental data points from Davis et al., Donnelly and Katz, and Pikaar illustrated for comparison. As can be seen from the figure, the agreement is very good except for the deviation in the Donnelly and Katz data described above. ProMax appears to also indicate that the Donnelly and Katz measurements are incorrect, as does the Davis et al. and Pikaar data. The average deviation, average absolute deviation, and maximum absolute deviation between the Davis et al. experimental values and ProMax predictions are -0.30°F (-0.17°C), 0.67°F (0.37°C), and 3.2°F (1.8°C), respectively. For the Pikaar data along the three phase locus, the average deviation is 0.08°F (0.04°C), the average absolute deviation is 0.45°F (0.25°C), and the maximum absolute deviation is 1.8°F (1.0°C). In both the Davis et al. and Pikaar data, the maximum deviations are near the maximum pressure in Figure 4, the same area where the Donnelly and Katz data deviate from the Davis et al. and Pikaar data. At this location, the discrepancy between the Davis et al. and Pikaar data is also the largest. At the lower pressures and temperatures, ProMax is normally within a fraction of a degree of the experimental measurement. ProMax is serving in a purely predictive role in this and the analyses that follow. Model parameters within ProMax have not been fit to any solid CO_2 system data.

In addition to the three phase locus, Figure 4 presents the predicted frost and freezing lines from ProMax for 1%, 3%, 5%, 10%, and 20% CO_2 in methane. The frost data of Pikaar acquired using
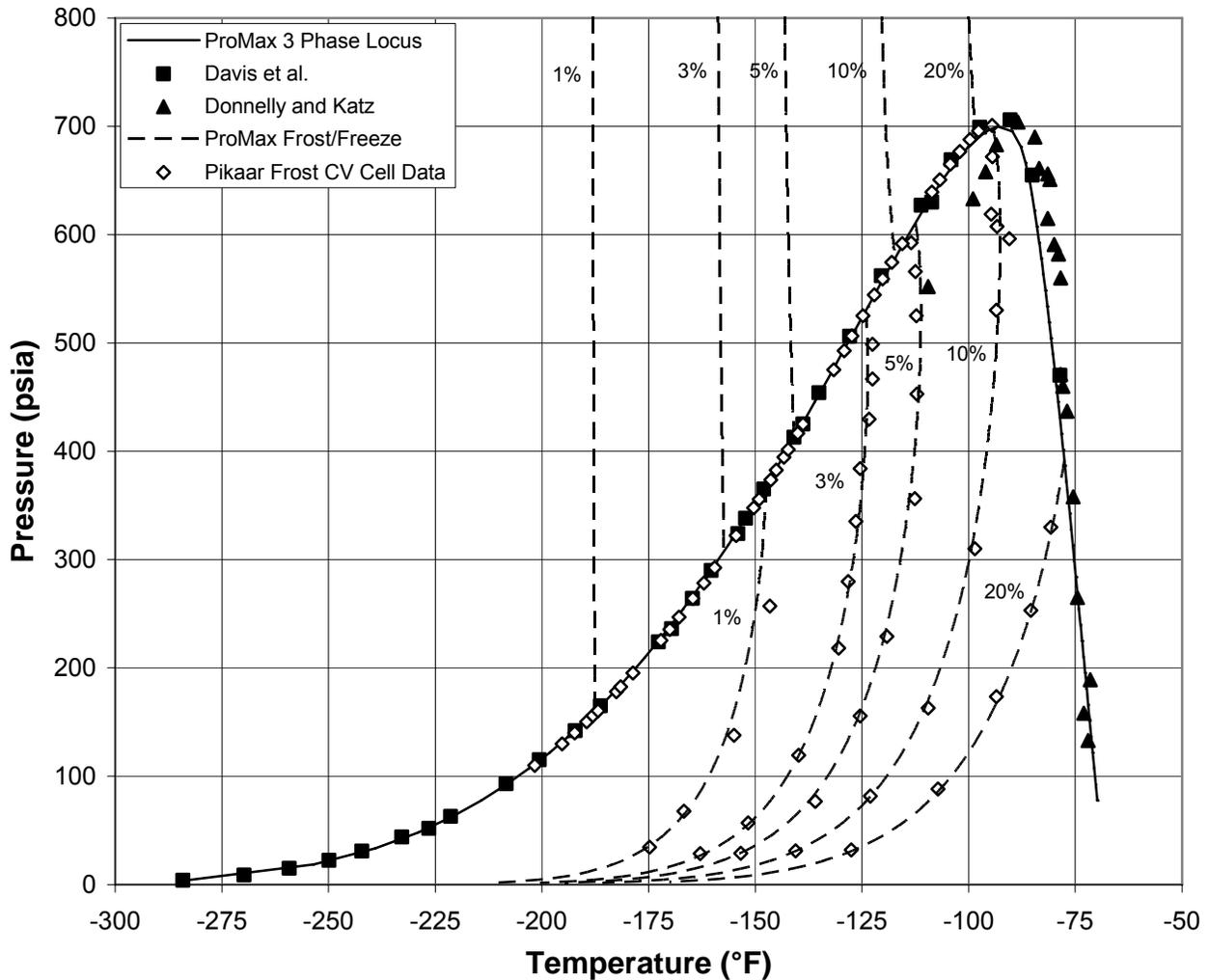
Figure 4. ProMax Three Phase Locus Compared to Experimental Data.

the constant volume cell apparatus are also presented on the same plot. Comparing the frost data to the ProMax predictions indicate the average deviation, average absolute deviation, and maximum absolute deviation are 0.08°F (0.05°C), 0.85°F (0.47°C), and 3.2°F (1.8°C), respectively. The experimental data and ProMax both indicate that at some compositions the frost data undergo retrograde sublimation, where an isothermal increase in pressure will cause the solid that is present to sublime. Pikaar did not measure any freezing data along these constant composition lines so only projections, no data points, are presented in that region.

Figure 5 presents the isothermal predictions of frost and freezing conditions in addition to the Pikaar data taken in the saturation cell apparatus. The three phase locus compositions of the vapor and liquid phases calculated by ProMax are also shown. Horizontal tie lines between the vapor and liquid compositions are drawn to tie the SVE region to the SLE region across the three phase region. It should be noted that the vapor and liquid compositions in this diagram are not at constant temperature as in most pressure-composition diagram presentations. The temperature of the tie lines is a direct function of the pressure due to the univariant nature of the three phase binary system.
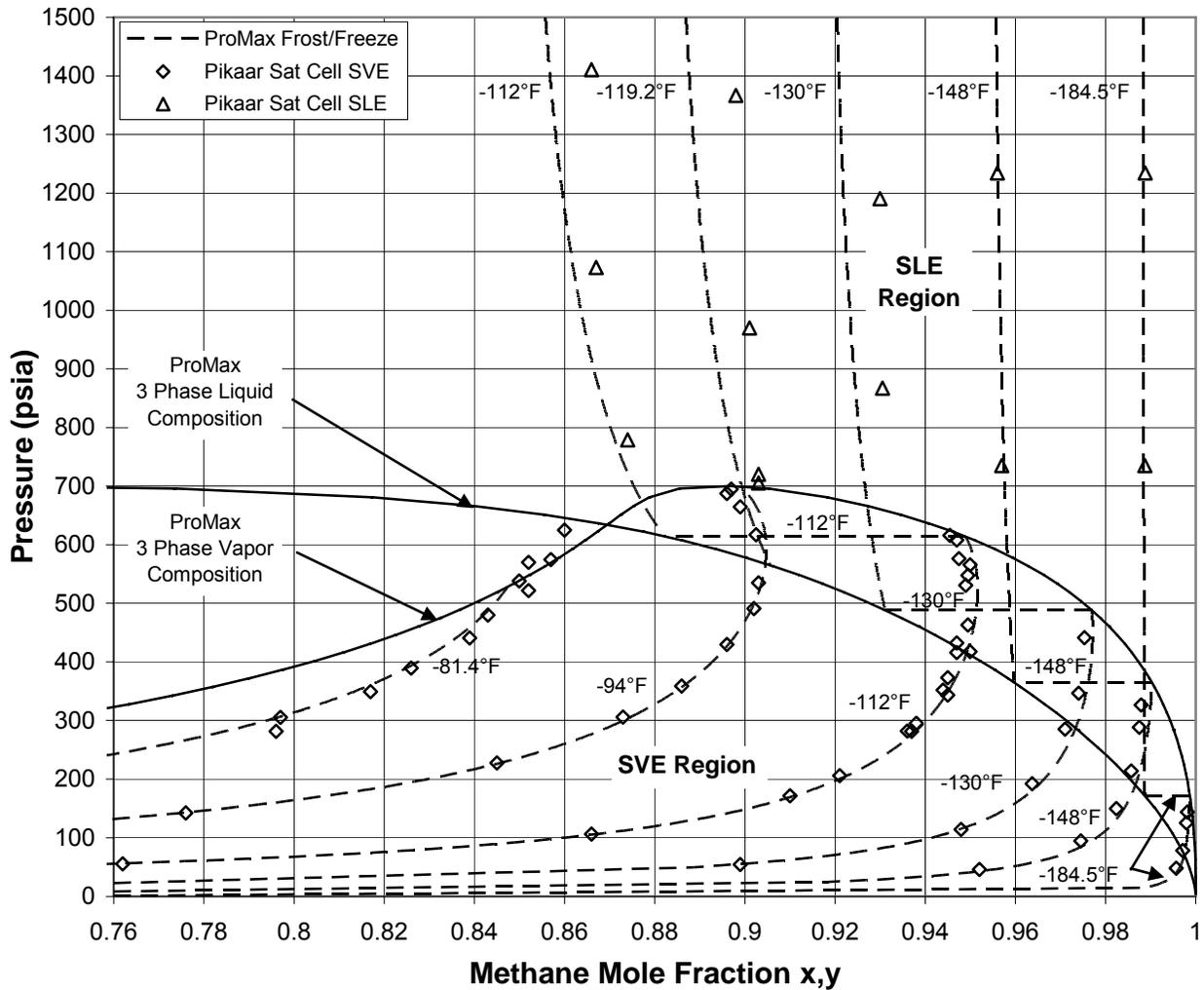
9

Figure 5. Pressure-Composition Diagram for the CH$_4$-CO$_2$ System in the Solid Region (Experimental Data from Pikaar [4]).

For the most part, the agreement with the experimental data is also quite good with this independent set of data. There is a discrepancy in the -81.4°F (-63°C) frost data at the highest methane composition point. This point leads Pikaar to draw the vapor composition line in his graphical presentation of saturation cell results concave down in this area. In fact, in the Pikaar thesis, the vapor composition is drawn concave down for the entire 80-100% methane composition range due to this measurement (Pikaar does not plot below 80% methane). Hwang et al. [8] used the Pikaar data in presentation of their dew point measurements. Hwang et al. appear to have directly copied without verification the vapor composition line from the Pikaar saturation cell results. If this single point is ignored, the line could have been drawn with the inflection point shown in Figure 5. The ProMax line is not generated using a single point, but is a continuous plot over the composition range presented in Figure 5. Donnelly and Katz also present a pressure-composition diagram that shows the same inflection as generated by ProMax in Figure 5. Their data extend to high CO$_2$ levels with several measurements to justify the inflection. The agreement of ProMax with the Donnelly and Katz data in

this region is good. While the Donnelly and Katz data have some discrepancies with other researchers, the discrepancies are at the low CO_2 end of the composition region, not the high end. It is interesting to note further that in a separate graphical comparison of his data to the Donnelly and Katz data, Pikaar draws the inflection point evident in Figure 5.

In addition to this disagreement with ProMax in Figure 5, disagreement exists between ProMax and the Pikaar data in the SLE region at the higher temperatures. The agreement at the lower temperatures is excellent. The maximum temperature disagreement between the Pikaar data and ProMax is 2.3°F (1.3°C). Other than the Pikaar data, we are only aware of four SLE points from the Donnelly and Katz data. A comparison of these data and ProMax is presented in Table 1. The average

Table 1. Comparison of ProMax Predictions to Donnelly and Katz Solid-Liquid Equilibrium Data [3].

Liquid Mole % CH$_4$	Pressure (psia)	Temperature (°F)	
		Experimental	ProMax
13.5	623	-75	-77.2
23.2	633	-79.5	-81.5
57.4	782	-88.5	-88.7
79.5	666	-109.5	-98 (700 psia)

difference in the data and predicted value is 1.5°F (0.8°C) if the final point is omitted from the analysis. There is significant disagreement with the final point. However, this point is in the same region where the Donnelly and Katz data disagree with other authors. In fact, the Pikaar SLE data indicate that the composition would need to be about 88% methane as opposed to the 79.5% reported value to achieve this low freezing point. Davis et al. also measure the same 79.5% liquid methane system on the three phase locus and their results indicate the temperature is -97.4°F at 699 psia, within 0.6°F of the predicted value from ProMax. Their measurement indicates the pressure would need to be at least this value to exist as a liquid of the stated composition. According to ProMax, the 666 psia value from Donnelly and Katz would form solid CO_2 at -86.6°F, which lies on the three phase locus with a liquid composition of about 45% methane. Since ProMax matches the higher temperature and CO_2 content data from Donnelly and Katz in the SLE region and because the isotherms in the SLE region are virtually at constant composition due to the relative incompressibility of the SLE system, it does not appear that the prediction departure increases with increasing temperature as may be implied by Figure 5.

A comparison of the predicted temperatures from vapor composition measurements given by Davis et al. is shown in Table 2. The vapor compositions were measured at locations along the three phase locus. The deviations are acceptable, especially if the first two points are removed from their computation. In Davis et al., a figure similar to Figure 4 is presented, but constant composition lines of 0.3% (SVE), 0.1% (SVE and SLE), and 0.03% (SVE) CO_2 are added and attributed to Pikaar [4]. However, Pikaar does not present such constant composition measurements in his thesis. The lowest constant composition line provided is 1% CO_2. The 0.1% line in Davis et al. intersects the three phase locus close to the temperature of the first point in Table 2 at approximately 100 psia. The only possible mechanism to obtain the 0.12% value or any composition close to it from the work of Pikaar is to read it graphically using measurements made in the saturation cell apparatus. This would indicate the three phase locus pressure to be approximate 155 psia which corresponds to a temperature of -188°F (-122°C), very close to the ProMax prediction. Further, if the first value in Table 2 was correct, we would expect large deviations in the solid-vapor region of Figure 5 as the -184.5°F isotherm

Table 2. Solid Formation Temperature Predictions for Davis et al. [5] Vapor Compositions Measured along the Three Phase Locus in the CO_2-CH_4 system.

Vapor Mole % CO_2	Temperature (°F)	
	Experimental	ProMax
0.12	-206.0	-185.9
0.63	-161.6	-156.6
1.08	-143.1	-145.9
1.72	-140.0	-136.3
2.79	-128.5	-125.8
3.67	-120.0	-119.7
5.65	-111.1	-109.6
11.73	-89.4	-88.9
Average. Deviation		-3.9
Average Absolute Deviation		4.6
Maximum Absolute Deviation		20.1
Average Deviation[*]		-1.0
Average Absolute Deviation[*]		1.9
Maximum Absolute Deviation[*]		3.7

[*]These deviations exclude the 0.12% and 0.63% predictions due to suspected errors in the measurements.

approached the vapor composition line. In fact, this is not observed providing additional evidence that the first experimental points are probably incorrect.

Table 3 presents a comparison of predicted solid formation temperatures using ProMax and PROSIM based on liquid phase composition measurements as given by Kurata [9] in GPA RR-10. RR-10 includes the Davis et al. data, in addition to data from other sources. For ProMax, the table indicates the -153.9°F and -168.0°F points contain the largest errors in the group. If the compositions for these two points are read from the Pikaar saturation cell graphs, the experimental results would be -156.5°F and -170.0°F, respectively, closer to the predicted values of ProMax.

Table 3 provides the same analysis as given by Eggeman and Chafin [1, 2]. From their reported values, it is apparent to us that Simulator B is our simulation program, PROSIM. ProMax was not available at the time of their paper. While ProMax generally offers improved predictions over PROSIM, especially for the low CO_2 content points, the deviations in Table 3 for PROSIM are different than those presented by Eggeman and Chafin. There, the reported maximum deviation for PROSIM of -28°F occurred in the 10.08% CO_2 point, with a corresponding predicted value of -90.8°F. Here, the deviation for the same point is -4.5°F. What is the cause of this reported difference?

The experimental data reported in Table 3 were obtained along the three phase locus. Consequently, the system is not in the SLE region but in the SVLE region. If the overall composition is specified using the experimental liquid composition, the only point that will match the experimental conditions in the space of pressure-temperature is the intersection of the freezing line with the three phase locus (see Figure 4). At that intersection, the liquid and overall compositions are equal, and the liquid is in equilibrium with a bubble point vapor. While pressure-temperature combinations of the three phase locus were published by the original authors of the GPA RR-10 data, the pressures corresponding to all of the experimental data compositions in Table 3 were not published due to the

Table 3. Solid Formation Temperature Predictions for GPA RR-10 [9] Liquid Compositions Measured along the Three Phase Locus in the CO_2-CH_4 system.

Liquid Mole % CO_2	Temperature (°F)		
	Experimental	**ProMax**	**PROSIM**
90.00	-73.9	-76.0	-75.9
86.50	-75.0	-77.7	-76.9
80.00	-77.0	-80.5	-78.7
76.80	-79.5	-81.7	-79.5
70.00	-81.0	-83.7	-81
60.00	-83.5	-85.9	-82.7
54.30	-86.0	-86.8	-83.5
50.00	-86.5	-87.5	-84.1
42.60	-88.5	-88.6	-85.2
20.50	-97.4	-97.8	-94.2
15.39	-105.2	-104.3	-101.7
10.08	-119.0	-117.0	-114.5
5.85	-131.8	-135.6	-135.1
2.94	-153.9	-158.0	-159.9
1.83	-168.0	-171.8	-175.5
0.93	-189.0	-189.4	-195.9
0.58	-199.5	-200.2	-208.8
0.37	-208.7	-209.7	-220.1
0.25	-216.3	-217.5	-229.3
0.16	-226.3	-225.9	-239.2
Average Deviation		1.5	2.8
Average Absolute Deviation		1.8	4.8
Maximum Absolute Deviation		4.1	13.0

univariant nature of the three phase binary system. In calculating the PROSIM values, Eggeman and Chafin obtained the pressures by calculating the bubble point pressure using the experimentally reported value of SVLE temperature. While this procedure does provide a VLE bubble point pressure that matches the experimental temperature, the procedure does not provide a pressure-temperature combination that is at the intersection of the SVLE locus and freezing line as predicted by the simulator. Only if the program perfectly predicted the experimental temperature would the calculated pressure be at this intersection. Normally, this does not represent a problem if the bubble point pressure is above the SVLE locus pressure due to the small change in freezing that occurs with pressure. Many of the reported values were at these higher pressures in their paper. However, if the bubble point pressure is below the SVLE locus pressure, even infinitesimally, the results can differ significantly, just as the actual system will change significantly if the pressure is lowered through the three phase locus.

Since Figure 2 includes a 10% CO_2 phase envelope superimposed on the three phase locus, the figure can be used as a tool to understand this phenomenon fully (assume insignificant changes between 10% and 10.08% CO_2). Using the experimental temperature of -119°F, an interpolation of the GPA RR-10 three phase locus data provides a pressure of approximately 572 psia. The bubble point

pressure predicted by ProMax for this composition is 563 psia. This pressure lies slightly below the three phase locus pressure from ProMax, and yields a predicted formation temperature of -92.5°F, a point on the SVE line, and close to the -90.8°F value provided by Eggeman and Chafin for PROSIM. Consequently, at first inspection, it appears that this point is significantly overpredicted by the program. Yet, if the pressure is increased to the three phase locus pressure of 580 psia, the predicted temperature is -117°F, the pressure-temperature coordinate of the SLE and SVLE intersection in ProMax. In calculating the values in Table 3, the system was at the intersecting pressure, thus providing the corrected predictions. This same issue was encountered in the 15.39% and 20.5% points in their paper.

Experimental errors in temperature, pressure, and composition measurement can aggravate the comparison further. Pikaar reports the 10% CO_2 SLE-SVLE intersection to be -115°F and 595 psia, unexpectedly higher in temperature than Davis et al. for a system than contains marginally less CO_2. The calculated bubble point pressure for this temperature by ProMax is 598 psia, very close to the Pikaar value. Consequently, the predicted SLE-SVLE intersection for this system by ProMax lies between the Pikaar and Davis et al. measurements, further justifying the 580 psia value and indicating the program is likely very accurate.

Calculation of dry ice conditions for this type of system requires sophisticated utilities and phase envelope routines such as those present in ProMax and PROSIM. As stated earlier, we cannot make any statements regarding the other simulators compared by Eggeman and Chafin [1, 2] because we cannot comment on the robustness of their utilities.

The reader is also further cautioned about the use of the constant composition approach proposed by Eggeman and Chafin [1, 2]. In the constant composition approach, the liquid or vapor composition is held constant while the temperature is adjusted to obtain equal component chemical potentials between the phase and the solid. Depending on the results and its application, the converged solution may be unknowingly thermodynamically unstable in some cases. For example, if the calculated solids formation temperature of the liquid is higher than the stage temperature of a distillation column, then solving the single equilibrium expression for temperature

$$\mu_{CO_2}^{L} = \mu_{CO_2}^{S} \tag{4}$$

at fixed liquid composition and pressure will not result in a system with minimum Gibbs free energy, a fundamental equilibrium requirement. This is due to the fact that at temperatures above the stage temperature, the liquid on the stage will partially vaporize since the liquid is at its bubble point temperature. A liquid at this elevated temperature with the original stage composition and pressure cannot exist. Above the stage temperature, the liquid will not form solid CO_2 at the pressure of the stage unless a portion of the liquid is vaporized. The calculation must consider the creation of the vapor phase and solve the full equilibrium expression

$$\mu_{CO_2}^{V} = \mu_{CO_2}^{L} = \mu_{CO_2}^{S} \tag{5}$$

for temperature, adjusting the composition of the vapor and liquid phases as required to maintain equilibrium and mass balance. Obviously this is a different set of equations and will result in a different solid formation temperature solution. As mentioned earlier, the creation of the vapor phase (or any other phase) lowers the Gibbs free energy of the system, resulting in a thermodynamically stable system. The formation of the vapor usually will prevent the solid CO_2 from forming at the temperature of the constant composition approach. Since the chemical potential and derivative related properties usually experience significant directional changes as phases are added or removed from a binary or multicomponent system, the mathematical difference between the solution of a

14

thermodynamically stable system and one that is unstable can be large. As shown in Figure 3, as the system becomes more pure in character, a genuine condition near the top of a demethanizer, these changes approach near first order transition with near derivative discontinuity at the phase boundary.

An analogous argument can be made for solid formation temperatures of vapors that are lower than the calculated stage temperature. Only if the predicted temperature is a thermodynamically stable condition will the values normally be accurate with the constant composition approach.

It also should be noted that GPSA Engineering Data Book [10] Figure 13-64 has the same caveats, because it is effectively a constant composition approach. The results are only valid if the phase in equilibrium with the solid truly exists at the temperature, pressure, and composition of the calculations. The procedure provides no mechanism to insure or check this condition, except for systems that are nearly pure methane. Consequently, any comparison of predicted results to GPSA Figure 13-64 must consider the possibility of thermodynamically unstable vapors or liquids in systems with more than insignificant amounts of CO_2.

If the constant composition approach was employed to calculate the freezing temperature of the 10.08% CO_2 liquid discussed above, the result would yield an SLE temperature near the experimental -119°F for pressures below the three phase locus (GPSA Figure 13-64 gives -116°F). In calculating this system, equation 4 would be solved exclusively. In reality, the system forms a frost near -92.5°F for these pressures as seen in Figure 2. No liquid would be present.

Multicomponent Mixtures

Multicomponent mixtures create additional complexities because the number of degrees of freedom increases with the additional components. There is no univariant solid-vapor-liquid three phase locus present in a multicomponent mixture. Therefore, the three phase condition is not restricted to a line in the pressure-temperature diagram as it was for a binary system.

In order to determine the quality of predictions for multicomponent systems, Figure 6 provides a comparison of the quaternary system of carbon dioxide, methane, ethane, and propane data from
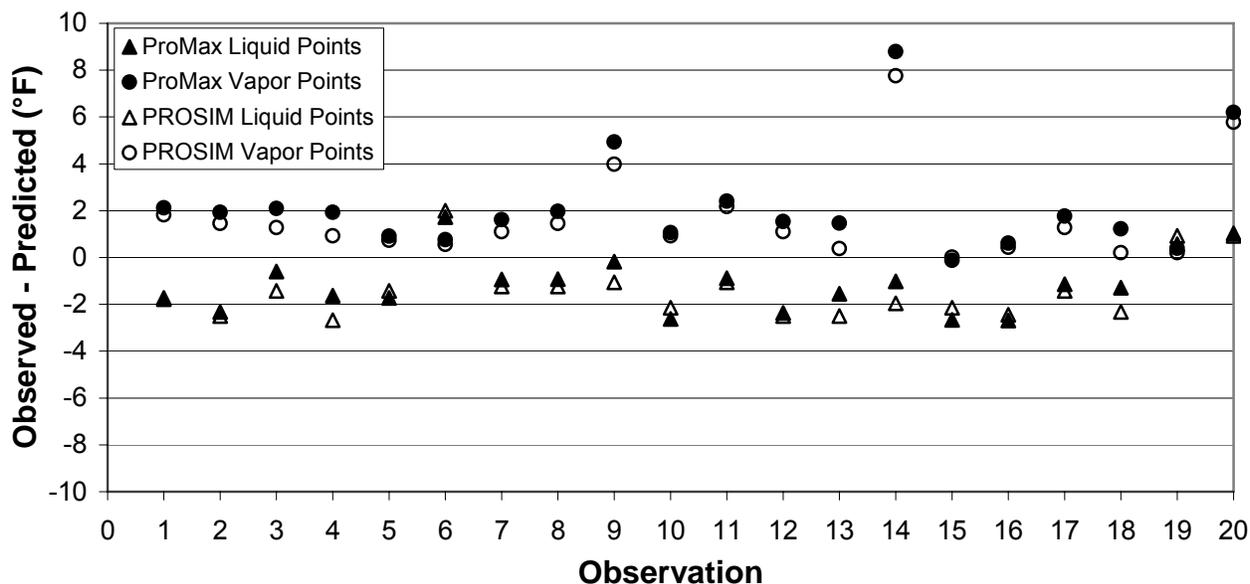

Figure 6. ProMax and PROSIM Residual Freezing Temperature Predictions for GPA RR-10 Quaternary Data [9].

15

GPA RR-10 to predicted values from ProMax and PROSIM. These data are in the three phase region, and include reported compositions for the liquid and vapor phases. The predictions can be made using both the vapor and liquid composition, since they are independently measured at the stated pressure. Using ProMax for the liquid composition calculations, the average deviation between the experimental and predicted value is -1.1°F (-0.6°C), the average absolute deviation is 1.5°F (0.8°C), and the maximum absolute deviation is 2.7°F (1.5°C). For the experimental vapor phase composition, the average deviation is 2.2°F (1.2°C), the average absolute deviation is 2.2°F (1.2°C), and the maximum absolute deviation is 8.8°F (4.9°C). The results for PROSIM are similar to ProMax with PROSIM being slightly better for the vapor phase. For both programs, the majority of the deviation for the vapor composition values was in a single point (observation 14). An analysis of the data presented in RR-10 indicates that this point is at the same pressure and nearly identical in composition to observation 13 in the data set. Yet, a 5.4°F (3°C) difference exists in the reported solid formation temperature between the two experimental points.   The error increase in observation 14 over observation 13 is essentially 5.4°F, a large portion of the 8.8°F maximum deviation. This difference results in a significant weighting of the error present in the deviation statistics.

In order to better understand the solid phase behavior of these multicomponent systems, consider the phase envelope generated by ProMax for the vapor, separated from its liquid, of observation 7 in the RR-10 data as presented in Figure 7. The composition of this vapor is 4.45% CO_2, 93.6% CH_4, 1.38% C_2H_6, and 0.57% C_3H_8. The experimental value for the incipient dry ice point is -117.4°F (-83.0°C) at a pressure of 300 psia (20.7 bar). The predicted value for the dry ice point is -119.0°F (-83.9°C), with a difference of 1.6°F (0.9°C) as seen in Figure 6. The phase envelope
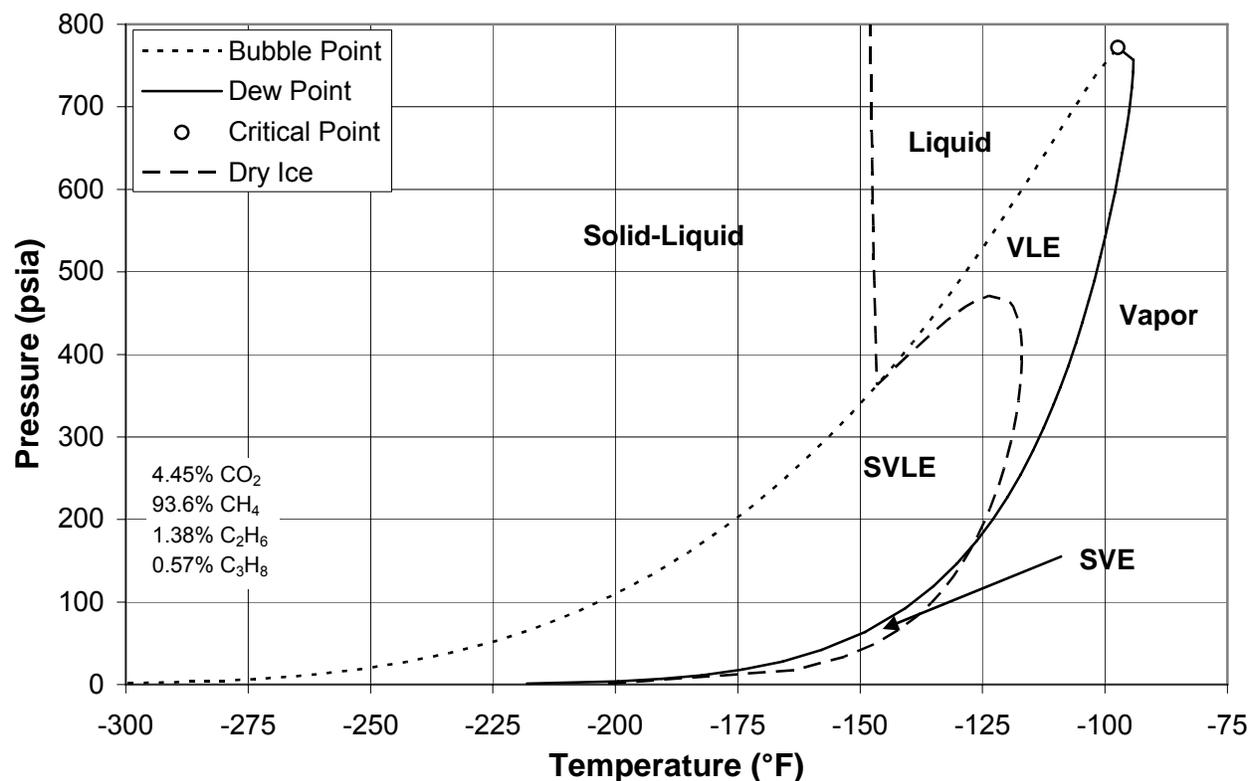

Figure 7.   Phase Envelope of Observation 7 for the Quaternary System Vapor Composition in GPA RR-10 [9].

illustrates that this point is in the SVLE region. At pressures between 375 and 470 psia (25.9 and 32.4 bar), the system exhibits three incipient dry ice points for a given pressure. Whether or not the system exhibits a pressure region that contains multiple dry ice points depends upon the overall system composition. Temperatures between the lowest and middle point comprise a solid free zone. Unlike the binary system, there is a region, not a line, of SVLE for the multicomponent mixture.

Phase Behavior of Hydrate Systems

Systems under hydrate formation conditions experience analogous phase behavior to those forming solid CO_2. Depending on the content of water and the composition of other compounds, multiple temperature zones of incipient hydrate formation at constant pressure may exist. This is particularly true for systems containing high acid gas compositions. The problem is even more complicated when inhibitors are present such as methanol where the system can form immiscible liquid phases. Figure 8 presents a phase diagram generated by ProMax of a system containing 83.15% CO_2, 12.38% CH_4, 1.96% C_2H_6, 1.66% C_3H_8, 0.37% i-C_4H_{10}, and 0.48% n-C_4H_{10} as measured by Adisasmito and Sloan [11]. In addition to the incipient anhydrous dry ice curve, the hydrate formation curves for water saturated and 7 lbm water/MMSCF (150 ppm) are shown. Here, the dry ice line and hydrate line under water saturated conditions do not have a pressure region that exhibits more than one incipient formation point. However, the 7 lbm/MMSCF H_2O hydrate line does experience this behavior between 280 to 465 psia (19.3 to 32.1 bar). This hydrate formation behavior has been discussed previously by Case et al. [12] and Sloan [13]. For the water saturated system, isobaric cooling of the system at 400 psia (27.6 bar) results in hydrate formation at temperatures below 44°F
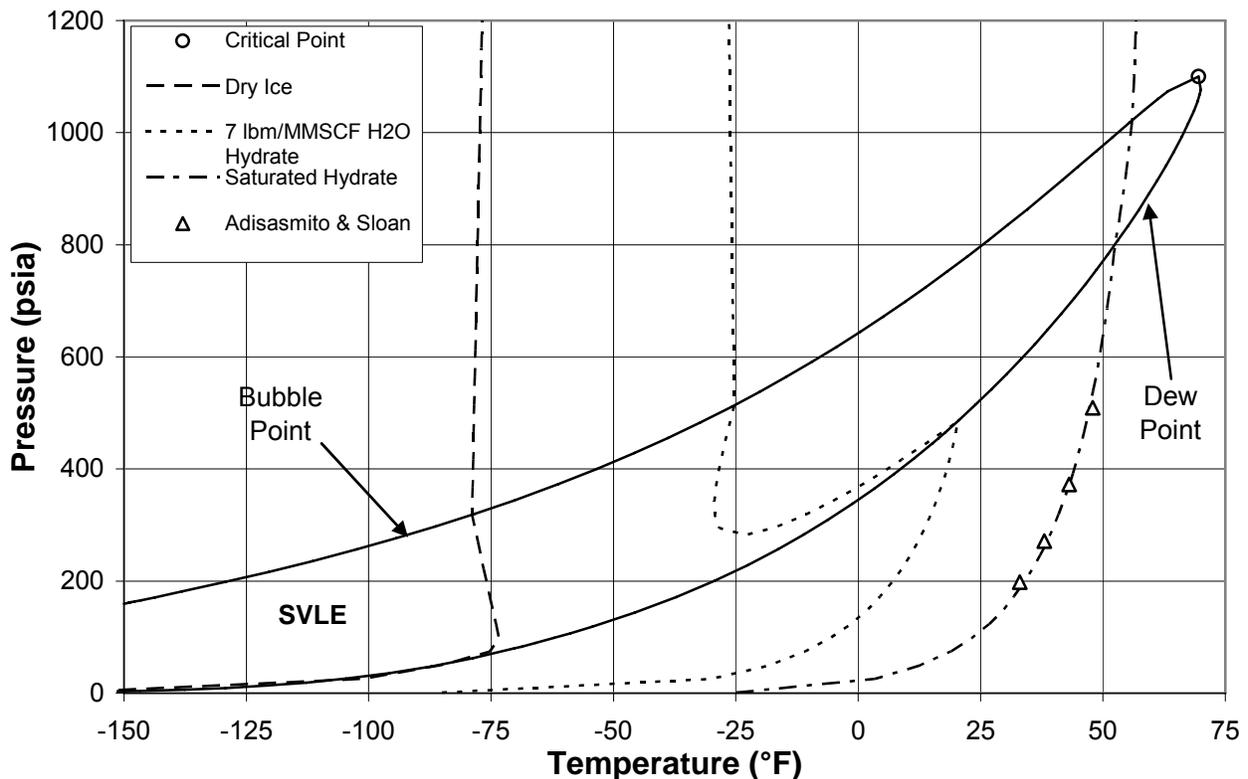

Figure 8. Predicted Dry Ice and Hydrate Formation for High CO_2 Content Mixture (Data from Adisasmito and Sloan [11]).

17

(6.7°C). For the system with 7 lbm/MMSCF, isobaric cooling at 400 psia results in hydrate formation at 18.1°F (-7.7°C). However, as cooling continues, the dew point line is intersected and liquid begins to form. The hydrate is dissolved by the liquid until no more hydrate exists at 5.9°F (-14.5°C). Further cooling causes a decrease in water solubility in the liquid as more liquid is formed until a temperature of -28.4°F (-33.6°C) is obtained. Below this temperature, the water forms a hydrate phase. As with CO_2 freezing presented in Figure 7, a region exists where lowering the temperature will eliminate hydrates from forming, rather than produce hydrates.

Table 4 presents a comparison of the predicted hydrate formation temperatures along the saturation line in Figure 8 to the Adisasmito and Sloan experimental measurements. The table indicates that good agreement exists with experimental data for this high acid gas multicomponent system. The average deviation between the experimental and predicted values is -0.23°F (-0.13°C), the average absolute deviation is 0.56°F (0.31°C), and the maximum absolute deviation is 0.97°F (0.54°C).

Table 4. Comparison of ProMax Predicted Hydrate Conditions to the High
CO_2 Content Data from Adisasmito and Sloan [11].

Pressure (psia)	Temperature (°F)	
	Experimental	ProMax
198	33.0	34.0
271	38.0	38.6
372	43.1	43.1
509	47.9	47.3

PRACTICAL IMPLICATIONS

As has been demonstrated by the foregoing discussion, used properly ProMax can provide an accurate representation of complex, solid forming systems. However, even with the warning indicating a solid formation condition the user defined threshold must be set carefully to achieve the optimum use of the simulation in plant design and troubleshooting.

For example, in a recent LNG liquefaction facility design, warnings were raised about the potential to form solid CO_2. This facility was small and did not have CO_2 removal on the inlet gas. The concern was that increasing concentrations of CO_2 could cause solids to plug the cold box and potentially cause problems in a turboexpander. After a careful check of the phase diagram against experimental data the design was released for construction. Only by using an understanding of the system gained from a careful analysis could this be done with confidence. The use of a warning indicating solid formation without understanding the system would have led to an overly conservative and expensive design.

In another recent example there was a concern about hydrate or ice formation in an operating column where water and hydrate inhibitors were present. By carefully analyzing the phase diagram on critical trays the engineer was able to confirm that solids would not form if the inhibitor concentration was kept in the correct range. In addition, this analysis led to an understanding and prediction of the distribution of the inhibitor in column products. The confidence gained by comparisons of ProMax against operating data led to operating changes which allowed stable operation closer to hydrate formation conditions than were found in the field without the aid of a simulation. This allowed the operator to reduce inhibitor injection to the minimum and cut operating costs.

It is important that the designer not only know and understand the phase diagram, but also that solid formation criteria must be carefully evaluated against critically evaluated experimental data such as that developed by GPA. Without such data it is impossible to know what kind of design margin provides an appropriate tolerance.

SUMMARY AND CONCLUSIONS

In this paper, we have attempted to describe the phase equilibria that are present in solid formation regions of systems in gas processing. We have shown that ProMax, the Bryan Research & Engineering, Inc. general purpose process simulator, and its predecessor PROSIM, accurately predict carbon dioxide freezing temperatures in binary systems with methane. We have shown similar accuracy with multicomponent mixtures as well. In the few cases where significant disagreement exists, suspect experimental data are present as compared with other researchers or other data within the same set. In general, the incipient formation temperature for dry ice is predicted to within approximately 2°F (1°C). We have also discussed the importance of knowledge of the phase behavior to safely utilize the results due to the multiplicity of roots that occur in some systems. The phase diagrams that have been presented illustrate that solids can form by raising the temperature or melt by lowering the temperature in certain regions. Finally, we have discussed concerns in calculating solid formation conditions using a constant composition approach, since this may yield results that do not represent true equilibrium.

ACKNOWLEDGEMENTS

REFERENCES CITED

1. Eggeman, T., and Chafin, S., "Pitfalls of CO_2 Freezing Prediction," *Proc. 82nd Annual GPA Convention*, San Antonio, TX, March 9-12, 2003.

2. Eggeman, T., and Chafin, S., "Beware the Pitfalls of CO_2 Freezing Prediction," *Chemical Engineering Progress*, 39-44, March, 2005.

3. Donnelly, H.G., and Katz, D.L., "Phase Equilibria in the Carbon Dioxide-Methane System," *Ind. Eng. Chem.*, **46**, 511, 1954.

4. Pikaar, M.J., "A Study of Phase Equilibria in Hydrocarbon-CO_2 Systems," Ph.D. Thesis, University of London, London, October, 1959.

5. Davis, J.A., Rodewald, N., and Kurata, F., "Solid-Liquid-Vapor Phase Behavior of the Methane-Carbon Dioxide System," *AIChE Journal*, **8**, 537-539, 1962.

6. Sterner, C.J., "Phase Equilibria in CO_2-Methane Systems," *Adv. Cryogenic Eng.*, **6**, 467-474, 1961.

7. Katz, D. L., private communication with Dan McCartney, 1974.

8. Hwang, S-C, Lin, H-m, Chappelear, P.S., and Kobayashi, R., "Dew Point Study in the Vapor-Liquid Region of the Methane-Carbon Dioxide System," *J. Chem. Eng. Data*, **21**, 493-497, 1976.

9. Kurata, F., "Solubility of Solid Carbon Dioxide in Pure Light Hydrocarbons and Mixtures of Light Hydrocarbons," GPA Research Report RR-10, Gas Processors Association, Feb., 1974.

10. *Engineering Data Book*, 11th ed., Gas Processors Suppliers Association, Tulsa, OK., 1998.

11. Adisasmito, S., and Sloan, E.D., "Hydrates of Hydrocarbon Gases Containing Carbon Dioxide," *J. Chem. Eng. Data*, **37**, 343-349, 1992.

12. Case, J.L., Ryan, B.F., and Johnson, J.E., "Water in high-CO_2 stream complicates design factors," *Oil & Gas Journal*, **83**, 103-107, May 13, 1985.

13. Sloan, E.D., *Clathrate Hydrates of Natural Gases*, Marcel Dekker, Inc., New York, 1990.